THE ASTROPHYSICAL JOURNAL, 206:728–734, 1976 June 15

8 TO 13 MICRON SPECTROPHOTOMETRY OF COMPACT SOURCES IN NGC 7538

S. P. WILLNER
Hale Observatories, California Institute of Technology and Carnegie Institution of Washington
Received 1975 October 9; revised 1975 November 24

ABSTRACT

Three infrared and radio sources in NGC 7538 have been observed with 1 percent spectral and 5″ spatial resolution. The very small southern source shows a deep silicate absorption feature at 9.7 μ while the northern extended source shows little or no silicate absorption, but has a 12.8 μ emission line from Ne II. The data imply that the compact source has a gas-to-dust ratio of 75 inside the ionized region. The extended source only 10″ away has a gas-to-dust ratio implied by the 10 μ data alone of 3×10^4, but the true ratio must be much lower to account for published 20 μ measurements.

Subject headings: infrared: sources — nebulae: individual

I. INTRODUCTION

The large optically visible H II region NGC 7538 contains three compact radio and infrared sources in an area 24″ by 24″. This area has been mapped at 5 GHz by Martin (1973) and at 2.2 and 20 μ by Wynn-Williams, Becklin, and Neugebauer (1974, hereafter WBN). Both the radio and infrared maps show three sources: IRS 1, 1″.5 in diameter, which is bright in the infrared but faint in the radio; IRS 2, 9″ in diameter, which is bright in the radio but fainter than IRS 1 at 10 μ; and IRS 3, 2″.7 in diameter, which has an energy distribution intermediate between those of IRS 1 and IRS 2 but is fainter than both at all wavelengths. Martin (1973) estimated upper limits for the ages of the compact sources of 4000 to 25,000 years from the radii of the H II regions and the speed of sound in ionized gas. An OH maser is associated with IRS 1 (Wynn-Williams, Werner, and Wilson 1974), and molecular emission from CO is found over a region nearly a degree in diameter (Wilson *et al.* 1974). Emission lines from H_2S (Thaddeus *et al.* 1972), CS (Turner *et al.* 1973), HCN (Morris *et al.* 1974), and H_2CO (Downes and Wilson 1974) have been detected from the area of the compact infrared and radio sources, and the brightest CO emission peak is at that position (Wilson *et al.* 1974).

Broad-band infrared measurements have shown that IRS 1 has a silicate absorption feature near 10 μ, while IRS 2 does not (WBN). Aitken, Jones, and Penman (1974) have obtained 8 to 13 μ spectra of several H II regions including NGC 7538. Their field of view included both IRS 1 and IRS 2 and showed a deep silicate absorption feature at wavelengths near 10 μ. Spectra of compact sources in other H II regions have been obtained by Gillett *et al.* (1975*a*, hereafter GFMCS). These spectra showed a silicate absorption feature and often an emission line of Ne II at 12.8 μ. The Ne line flux generally indicated a Ne II abundance below the cosmic abundance of neon.

In this paper, observations which spatially separate the three compact sources with spectral resolution $\Delta\lambda/\lambda = 0.01$ from $\lambda = 7.4$ to 13.5 μ are presented. The instrument and observing techniques are described in § II. Section III describes observations of emission lines in IRS 2. Models fitted to the observed emission are presented in § IV, various source parameters are derived, and the masses of the compact H II regions and their gas-to-dust ratios are estimated and interpreted. An estimate is also made of the mass of the material shown to be present around IRS 1. Section V summarizes the results.

II. OBSERVATIONS

The spectrometer uses a liquid nitrogen cooled circular variable filter as the wavelength selective element. A barium fluoride Fabry lens images the primary of the telescope onto an arsenic-doped silicon detector, which is cooled with liquid helium. Observations are made by setting the wavelength, integrating using normal infrared chopping and beam switching techniques, and advancing to the next wavelength. The wavelengths measured are separated by 0.117 μ, which is slightly larger than the spectral resolution of 1 percent of the wavelength over most of the spectral range. Normally, measurements are made at every second wavelength step; then the filter is returned to the start, and measurements are made at the wavelengths which were skipped the first time. This procedure acts as a check on possible systematic errors due to guiding, changing atmospheric extinction, or changing instrumental sensitivity.

Most of the observations reported here were made on 1974 August 31 to September 4 and November 11 and 14 with the 2.5 m Hooker telescope. The August/September observations used a 5″ aperture and a 20″ beam separation in declination, while the November observations used a 7″.5 aperture and a 17″.5 separation in declination. The flux of IRS 1 was independent of aperture so all the measurements of it were averaged. The flux of IRS 2 increased by 0.39 ± 0.05 magnitudes with the larger aperture; the observations of it were corrected to a 5″ aperture

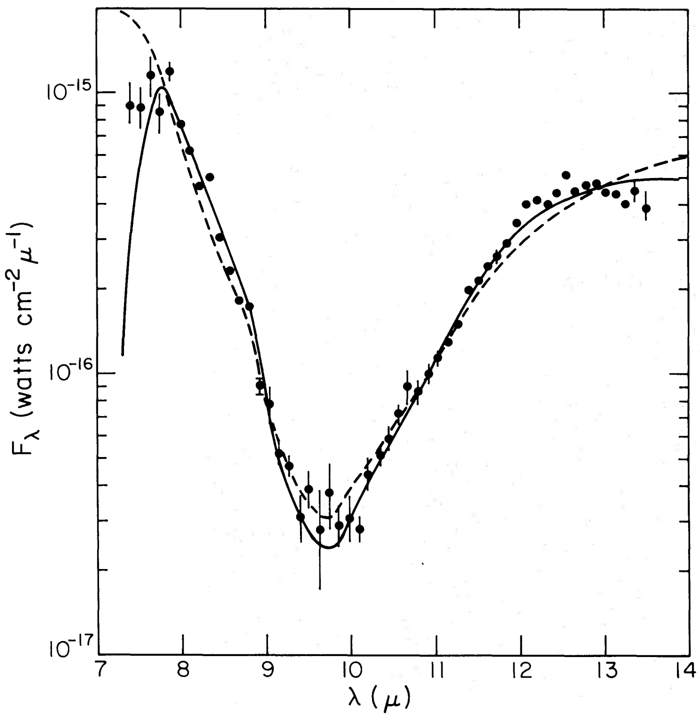

FIG. 1.—8 to 13 μ spectra of IRS 1. Error bars are given for the points with larger errors than 5%. The solid line is the spectrum predicted by the model with Trapezium-like emissivity, and the dashed line is that for blackbody emissivity.

before averaging. IRS 3 was observed only with the 5″ aperture. The results are shown in Figures 1 and 2.

The instrumental sensitivity as a function of wavelength was determined by measuring standard stars and the limb of the Moon. The Moon was assumed to radiate as a 350 K blackbody, which was found to be consistent with the hot stars having a Rayleigh-Jeans spectrum. An attempt was made to observe the standards and the objects at the same air mass, and residual differences in atmospheric extinction were compensated for in the data reduction using absorption parameters from Goldman (1970) for ozone and from McClatchey *et al.* (1972) for other gases. Absolute calibration was provided by observing α Tauri and assuming its flux at 10.1 μ is 1.91×10^{-15} W cm^{-2} μ^{-1}, consistent with the Caltech broad-band photometry.

In the spectra presented here, points near 12.8 μ, the wavelength of the Ne II line, were observed in succession in order to minimize systematic errors in measuring the line flux. These points were repeatedly measured on different nights as a further check on their accuracy. At other wavelengths, consecutive points were observed on different nights as a check on possible calibration errors.

Additional observations at wavelengths near 8.99 and 10.53 μ were obtained on 1975 June 20 and 21, in order to search for the predicted Ar III and S IV emission lines. The lines were not found, and the 3 σ upper limits are given in Table 1, along with the measurement of the Ne II line at 12.8 μ.

III. EMISSION LINES

The spectra presented in Figures 1 and 2 show that a strong Ne II line is present at 12.8 μ in IRS 2 but is absent in IRS 1. The nominal wavelengths, identifications, and the fluxes in this line and the upper limits on two other possible emission lines in IRS 2 are given in Table 1. The data for IRS 3 are insufficient to detect any emission lines.

The abundance of Ne II relative to H II for IRS 2 and an upper limit for IRS 1 can be derived using the formulation of Petrosian (1970); the results are given in Table 2. The 12.8 μ flux has been corrected for absorption by dust as discussed below. The Ne II abundance in IRS 2 is slightly below the cosmic abundance of neon, but this is easily accounted for if some of the neon is doubly ionized, as suggested by GFMCS for other H II regions. Because the infrared continuum flux from IRS 1 is large compared with the radio flux, the measurements do not imply any difference in the Ne II abundance in the two sources.

IV. SILICATE FEATURE

The prominent absorption feature from 8 to 12 μ in IRS 1 shown in Figure 1 is of the same type as that identified as due to silicates in the Becklin-Neugebauer point source in the Orion Nebula, the galactic center, and numerous sources in other H II regions (GFMCS and references therein). The feature in IRS 1 is one of the strongest such absorptions known, and indicates that a large amount of relatively cold dust lies along

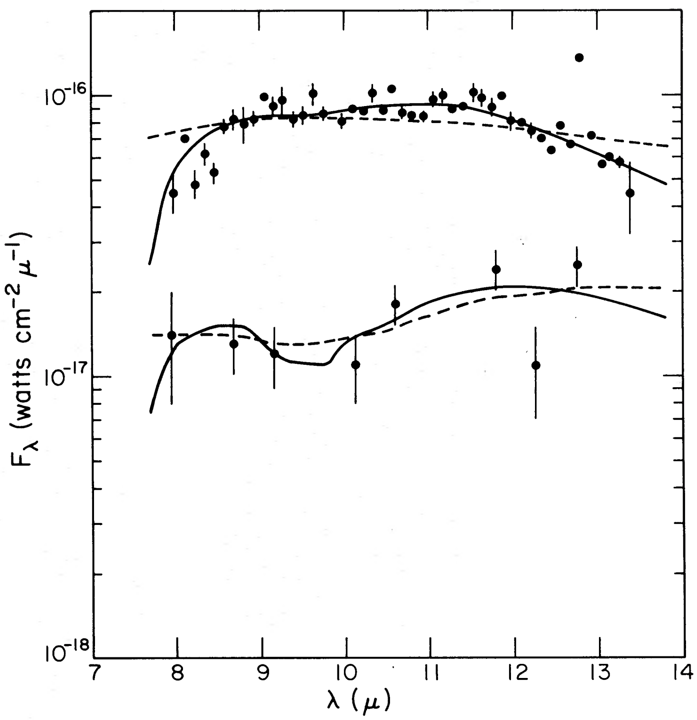

FIG. 2.—8 to 13 μ spectra of IRS 2 (*upper*) and IRS 3 (*lower*). See the legend for Fig. 1.

the line of sight to IRS 1. Because no feature of comparable strength is seen in IRS 2 or IRS 3, which are only 10″ away, the cold dust must be directly associated with IRS 1.

The quantities which can be most directly derived from the observations are the mass of emitting dust, its temperature, and the column density of absorbing dust in front of IRS 1. These quantities were calculated assuming that the emitting dust particles are all at the same temperature and are in a separate region behind a layer of absorbing silicate dust. The observed flux can then be fitted to a function of wavelength λ of the form

$$F_\lambda = \Omega\epsilon(\lambda)B_\lambda(T_d)e^{-\tau(\lambda)}, \quad (1)$$

where B_λ is the Planck function and ϵ is the emissivity. The absorption optical depth $\tau(\lambda)$ was assumed to be proportional to F_λ(Trapezium)/$B_\lambda(T_T)$, where F_λ(Trapezium) is the flux from the Trapezium (Forrest, Gillett, and Stein 1975), and T_T is an assumed temperature of the Trapezium. The parameters derived

TABLE 1

POSSIBLE EMISSION LINES IN IRS 2

λ	Identification	Measured Flux (10^{-18} W cm^{-2})	Corrected Flux (10^{-18} W cm^{-2})
9.04..........	Ar III λ8.99	< 1.1	< 3.4
10.57..........	S IV λ10.53	< 1.3	< 4.0
12.79..........	Ne II λ12.78	9.0 ± 0.9	14

TABLE 2

NEON ABUNDANCE

Object	Radio Flux* (10^{-26} Wm^{-2} Hz^{-1})	Measured 12.8 μ Flux (10^{-18} W cm^{-2})	Corrected 12.8 μ Flux (10^{-18} W cm^{-2})	log [N(Ne II)/N(H II)]
IRS 1.........	0.12	< 4.4	< 30	< −3.0
IRS 2.........	1.4	9.0 ± 0.9	14	−4.4

* From Martin 1973.

TABLE 3

BEST FIT MODEL PARAMETERS

		MODEL WITH TRAPEZIUM-LIKE EMISSIVITY				MODEL WITH BLACKBODY EMISSIVITY			
OBJECT	N	Ω (arcsec^2)	T_d (K)	$\tau(9.7)$	$\chi^2/N - 3$	Ω (arcsec^2)	T_d (K)	$\tau(9.7)$	$\chi^2/N - 3$
IRS 1...........	53	2.6×10^{-1}	370 ± 40	6.4 ± 0.3	4.0	5.4×10^{-2}	330 ± 30	4.2 ± 0.2	9.0
IRS 2...........	46	2.7×10^{-2}	270 ± 20	1.4 ± 0.2	2.7	4.1×10^{-3}	290 ± 20	0	6.1
IRS 3...........	8	1.6×10^{-2}	250 ± 50	2.4 ± 0.8	1.8	3×10^{-3}	250 ± 50	0.6 ± 0.7	1.8

from the model fit are the temperature T_d of the emitting dust, the peak optical depth $\tau(9.7)$ of the absorbing dust, and the effective solid angle Ω. Details of the model are in the Appendix.

The same two models for the emissivity $\epsilon(\lambda)$ of the hot dust were used as were employed by GFMCS. The first model, that of Trapezium-like emission, sets $\epsilon(\lambda) \propto F_\lambda(\text{Trapezium})/B_\lambda(T_T)$. The second model, that of blackbody emission, sets $\epsilon(\lambda) = 1$. Models such as $\epsilon(\lambda) \propto \lambda^{-1}$ or other smooth functions of wavelength generally give the same accuracy of fit to the observations as the blackbody emission model but with a different T_d.

The best fit model parameters are shown in Table 3. The calculated fluxes for Trapezium-like emissivity are shown as solid lines and for blackbody emissivity as dashed lines in Figures 1 and 2. The models do not seem to deviate from the observations in any systematic way, except that the very shortest wavelength observations of IRS 1 indicate an emissivity larger than that of the Trapezium. For all models the residuals from the model fit are larger than would be expected if only the observational statistical errors are considered. This is probably mostly due to the inaccuracy of the assumptions of a single temperature and Trapezium-like emissivity on which the models are based.

For both IRS 1 and IRS 2, Trapezium-like emissivity provides a much better fit to the data than blackbody emissivity; this conclusion is in agreement with that of GFMCS for other objects. In particular, for IRS 2, the best fit assuming blackbody emissivity had $\tau(9.7) = -0.4 \pm 0.2$, which is physically unreasonable. Therefore, all further discussions are based on Trapezium-like emissivity.

The visual extinctions to IRS 1, 2, and 3 can be crudely estimated from the depth of the silicate absorption. The extinctions are 90, 20, and 34 mag, respectively, if $A_V/\tau(9.7) = 14$ (Gillett *et al.* 1975*b*). These are consistent with IRS 1 and 3 being invisible on the Palomar Sky Survey red plates. A nebulosity does appear at the position of IRS 2 (WBN); the radio observations (Martin 1973) imply that the Hα surface brightness should be 13 mag arcsec^{-2}, and thus $A_{\text{H}\alpha} < 8$ mag and $A_V < 11$ mag. One explanation for the discrepancy between the low values of A_V implied by the short wavelength observations and the value of 20 mag implied by the 10 μ observations is that the dust is distributed nonuniformly in front of IRS 2, so that some parts of the nebula are heavily extinguished, while other parts are extinguished hardly at all. Persson and Frogel (1974) have suggested that this is the case in K3-50, which also has a large silicate absorption but comparatively small visual extinction.

The mass of emitting dust in the H II regions can be obtained from the models described above if the emission is optically thin, because the effective solid angle is directly proportional to the mass of emitting dust and its opacity per unit mass and inversely proportional to the square of the distance. That the emission is optically thin is shown in Table 4 which gives the emission optical depth $\tau_{\text{em}}(9.7)$ calculated from the effective solid angles derived from the model fits and from the radio diameters $\theta_{\text{H II}}$ of Martin (1973). The values of the mass of emitting dust M_d are also given in Table 4; the dust absorption coefficient $\kappa(9.7)$ has been taken as 3×10^3 cm^2 g^{-1} (Gillett and Forrest 1973) and the distance as 3.5 kpc (Israel, Habing, and de Jong 1973). The values of M_{gas}, the mass of ionized gas, are from Martin (1973), scaled to a distance of 3.5 kpc, and reduced by 40 percent in IRS 2 to allow for the small aperture. Table 4 also gives the calculated gas-to-dust ratios for the H II regions; it has been assumed that the infrared emission comes from the ionized region.

The gas-to-dust ratios of 3×10^4 and 10^3 indicated by the 10 μ data for the ionized regions of IRS 2 and IRS 3 are larger than the accepted interstellar value of 100 but comparable to the values found by GFMCS for other H II regions. These values are upper limits, because if there is dust present at much lower temperatures than those found from the model fit, such dust will not emit significantly between 8 and 13 μ and will therefore not contribute to Ω. In fact, the 20 μ flux from IRS 2 (WBN) is larger than would be predicted from the temperature of 270 K found here, and the 20 μ to 13 μ color temperature is 130 K. The corrections for silicate absorption at 13 μ and to the broad-band 20 μ measurement should be approximately equal (Knacke and Thomson 1973). It is impossible to deduce the true gas-to-dust ratio without knowing the details of the temperature distribution of the dust, but a normal interstellar ratio of 100 appears consistent with the observations. IRS 3 also has a larger 20 μ flux than would be predicted from the 10 μ observations, and the observations are compatible with a normal gas-to-dust ratio in this object.

The arguments above would be invalid if a substantial part of the 20 μ flux comes from outside the H II region. Some flux might originate, for example, in the cold material which produces the absorption at 10 μ and the emission at far-infrared wavelengths. Any

TABLE 4

CLOUD MASSES AND GAS-TO-DUST RATIOS

Source	Ω (arcsec^2)	M_d ($M_\odot$)	$\theta_{\text{H II}}$* (arcsec)	$\tau_{\text{em}}(9.7)$	M_{gas}* ($M_\odot$)	M_{gas}/M_d	N_{H} (atoms cm^{-2})
IRS 1.....	2.6×10^{-1}	1.2×10^{-4}	1.5	1.5×10^{-1}	9×10^{-3}	75	1.3×10^{23}
IRS 2.....	2.7×10^{-2}	1.2×10^{-5}	9	1.4×10^{-3}	3.6×10^{-1}	3×10^4	3×10^{22}
IRS 3.....	1.6×10^{-2}	7×10^{-6}	2.7	3×10^{-3}	9×10^{-3}	1×10^3	5×10^{22}

* From Martin 1973, corrected to $d = 3.5$ kpc.

such contribution is probably small, because in IRS 2 the 20 μ and radio maps are in good agreement, and in IRS 1 (see below) the 20 μ flux is no larger than is obtained by extrapolating the 8 to 13 μ flux.

The energy distribution of IRS 1 is different from that of IRS 2 and IRS 3 in that the 20 μ flux is much less relative to the 10 μ flux. The 20 μ, 13 μ, and 5 μ fluxes all fit a 370 K blackbody, the same temperature as derived from the 10 μ alone. The extinction at 5 μ should be about equal to that at 13 μ assuming $A_V/\tau(9.7) = 14$ (Gillett *et al.* 1975*b*) and a normal interstellar extinction law (Johnson 1968). It therefore seems that the assumption of a single temperature is reasonable for IRS 1, and the derived gas-to-dust ratio of 75 is accurate.

The absorption optical depth obtained from the model fit can be used to calculate the column density of material in front of the H II region. The column density can then be used to estimate the total mass outside the H II region. The column density of hydrogen atoms $N_H = f\tau(9.7)/\kappa(9.7)M_H$ where f is the gas-to-dust ratio in the cold medium outside the H II region and M_H is the mass of a hydrogen atom. The values of N_H for $f = 100$ are given in Table 4.

The relation between N_H and the total mass outside the H II region is strongly dependent on how the mass is distributed. The spherically symmetric density distribution requiring the least mass consistent with the measured column density is that in which all the mass is in a thin shell just outside the H II region. This mass is 2 $M_\odot$ for IRS 1. If the material is spread out, the total mass required is larger. For example, if the density $\rho(r) \propto r^{-2}$ from the radius of the H II region r_0 to some maximum radius r_1, the total mass is increased by a factor r_1/r_0. Because the absorption in front of IRS 2 is small, r_1 is less than the distance from IRS 1 to IRS 2. If the projected distance is comparable to the actual distance, the mass is 10 times greater or 20 $M_\odot$.

The effect of the silicate absorption in front of IRS 1 is to remove the energy at 10 μ and reemit it around 100 μ. As discussed above, the 5, 13, and 20 μ fluxes from IRS 1 fit on a 370 K blackbody, so if there were no absorption, most of the luminosity of IRS 1 would emerge around 10 μ. The minimum luminosity of $4 \times 10^4 L_\odot$ is obtained by assuming that there is no absorption at wavelengths shorter than 8 μ or longer than 3 μ. If it is assumed that the absorption at 5, 13, and 20 μ is 0.3 of that at 9.7 μ, the luminosity of IRS 1 corrected for absorption would be $2.4 \times 10^5 L_\odot$. If, as suggested by the model fits, the underlying spectrum of IRS 1 has a silicate emission feature, the luminosity would be $3 \times 10^5 L_\odot$. Any of the above luminosities is consistent with a far-infrared measurement by Harper and Thronson (1975) with a field of view which includes all three sources. If a luminosity of $3 \times 10^5 L_\odot$ is produced by a zero-age main-sequence star, it is of spectral type O6 (Panagia 1973) and mass 35 $M_\odot$ (Cester 1965). Such a star would produce 100 times more ionizing photons than are indicated by the radio observations. Depending on the unknown ratio between the ultraviolet and 9.7 μ optical depths, an optical depth high enough to absorb 99 percent of the ultraviolet photons may be consistent with the 9.7 μ optical depth of 0.15 inside the ionized region. Another possibility is that the energy of IRS 1 is supplied by a supergiant star; its spectral type is then B0.5, and only 3 times more ionizing photons are produced than would be derived from the radio observations. In either case it appears that a star of 35 $M_\odot$ has formed out of a condensation having total mass between 37 and 55 $M_\odot$.

V. CONCLUSION

The three compact sources in NGC 7538, identified by Martin (1973) as young H II regions, have spectra of two types. IRS 1 has a strong silicate absorption, while IRS 2 and IRS 3 have much weaker silicate absorption. The emission from IRS 1 from 5 to 20 μ can be explained with a single temperature for the emitting dust, but in IRS 2 and IRS 3 a range of temperatures is required. The gas-to-dust ratio of IRS 1 appears to be normal; the observations are probably consistent with normal ratios in IRS 2 and IRS 3. If older H II regions are dust depleted, the depletion must occur at a later stage of their evolution and is not an initial condition.

It is a pleasure to thank E. E. Becklin and G. Neugebauer for their support and encouragement, including many valuable comments on the manuscript, and C. Sarazin for a discussion of dust depletion mechanisms. S. V. W. Beckwith helped with the observations. This work was supported by National Aeronautics and Space Administration grant NGL 05-002-207 and National Science Foundation grant MPS 74-18555.

APPENDIX

In the approximation that the emitting dust particles in a source are all at the same temperature, the observed flux can be written as

$$F_\lambda = \Omega \frac{\epsilon(\lambda)}{\epsilon(9.7)} B_\lambda(T_d) \exp\left[-\tau(9.7)\frac{F_\lambda(\text{Trapezium})B_{9.7}(T_T)}{F_{9.7}(\text{Trapezium})B_\lambda(T_T)}\right] \quad (2)$$

(GFMCS). Here $\epsilon(\lambda)$ is the emissivity, and T_d is the temperature of the hot dust, $\tau(9.7)$ is the absorption optical depth at 9.7 μ, F_λ(Trapezium) is the flux from the Trapezium, T_T is the temperature of the dust in the Trapezium, and B_λ is the Planck function. There are four free-parameters: Ω, the effective solid angle; T_d; $\tau(9.7)$; and T_T.

F_λ(Trapezium) was taken from Forrest, Gillett, and Stein (1975). GFMCS found $T_T = 250$ K, but $T_T = 225$ K was used here for reasons discussed below. The applicability of the above model is discussed by GFMCS.

It was found that the only case in which T_T significantly affected the quality of the fit was that for IRS 1 using Trapezium-like emissivity. In this case, $T_T = 225$ K was at least 2 σ better than either 200 K or 250 K. The emissivity of dust as a function of wavelength is known to be different for different objects (Forrest, Gillett, and Stein 1975), and T_T should be regarded as a parameter describing the emissivity of the dust rather than as a physical temperature of the Trapezium. The lower value of T_T found here implies that the emissivity at 7 to 9 μ of the dust in NGC 7538 is larger than that in most of the H II regions studied by GFMCS.

The errors given for T_d and $\tau(9.7)$ are those corresponding to a unit rise in chi-squared per degree of freedom. This corresponds to the standard deviation rather than the standard deviation of the mean and should be a better estimate of the error when, as here, the error is not primarily statistical. This method of estimating the error in T_d and $\tau(9.7)$ should be accurate because T_d and $\tau(9.7)$ are not correlated. T_d does depend on T_T, and Ω depends strongly on T_d. Increasing T_T by 25 K increases Ω by about a factor of 3.

REFERENCES

Aitken, D. K., Jones, B., and Penman, J. 1974, in H II *Regions and the Galactic Centre: Proceedings of the Eighth ESLAB Symposium*, European Space Research Organization, ed. A. F. M. Moorwood, p. 43.
Cester, B. 1965, *Zs. f. Ap.*, **62**, 191.
Downes, D., and Wilson, T. L. 1974, *Ap. J.* (*Letters*), **191**, L77.
Forrest, W. J., Gillett, F. C., and Stein, W. A. 1975, *Ap. J.*, **195**, 423.
Gillett, F. C., and Forrest, W. J. 1973, *Ap. J.*, **179**, 483.
Gillett, F. C., Forrest, W. J., Merrill, K. M., Capps, R. W., and Soifer, B. T. 1975*a*, *Ap. J.*, **200**, 609 (GFMCS).
Gillett, F. C., Jones, T. W., Merrill, K. M., and Stein, W. A. 1975*b*, *Astr. and Ap.*, **45**, 77.
Goldman, A. 1970, *Appl. Optics*, **9**, 2600.
Harper, D. A., and Thronson, H. A. 1975, private communication.
Israel, F. R., Habing, H. J., and de Jong, T. 1973, *Astr. and Ap.*, **27**, 143.
Johnson, H. L. 1968, in *Nebulae and Interstellar Matter*, ed. B. M. Middlehurst and L. H. Aller (Chicago: University of Chicago Press), p. 193.
Knacke, R. F., and Thomson, R. K. 1973, *Pub. A.S.P.*, **85**, 341.
Martin, A. H. M. 1973, *M.N.R.A.S.*, **163**, 141.
McClatchey, R. A., Fenn, R. W., Selby, J. E. A., Volz, F. E., and Garing, J. S. 1972, *Optical Properties of the Atmosphere* (3d ed.; AFCRL report 72-0497).
Morris, M., Palmer, P., Turner, B. E., and Zuckerman, B. 1974, *Ap. J.*, **191**, 349.
Panagia, N. 1973, *A.J.*, **78**, 929.
Persson, S. E., and Frogel, J. A. 1974, *Ap. J.*, **188**, 523.
Petrosian, V. 1970, *Ap. J.*, **159**, 833.
Thaddeus, P., Kutner, M. L., Penzias, A. A., Wilson, R. W., and Jefferts, K. B. 1972, *Ap. J.* (*Letters*), **176**, L73.
Turner, B. E., Zuckerman, B., Palmer, P., and Morris, M. 1973, *Ap. J.*, **186**, 123.
Wilson, W. J., Schwartz, P. R., Epstein, E. E., Johnson, W. A., Etcheverry, R. D., Mori, T. T., Berry, G. G., and Dyson, H. B. 1974, *Ap. J.*, **191**, 357.
Wynn-Williams, C. G., Becklin, E. E., and Neugebauer, G. 1974, *Ap. J.*, **187**, 473 (WBN).
Wynn-Williams, C. G., Werner, M. W., and Wilson, W. J. 1974, *Ap. J.*, **187**, 41.

S. P. WILLNER: University of California, San Diego, Physics Department, C–011, La Jolla, CA 92093